29th Congress of the International Council of the Aeronautical Sciences
St. Petersburg, Russia; September 7–12, 2014

PREDICTION OF OPERATIONAL CHARACTERISTICS OF FLUID-FILM AND GAS BEARINGS FOR HIGH-SPEED TURBOMACHINERY USING COMPUTATIONAL FLUID DYNAMICS

Ravikovich Y.A.*, Ermilov Y.I.*, Pugachev A.O.*, Matushkin A.A.*, Kholobtsev D.P.*
***Moscow Aviation Institute (National Research University), Moscow, Russia**

Keywords: *hydrodynamic and hydrostatic lubrication, CFD, caviation, journal attitude curve*

Abstract

The analysis is presented for the computational fluid dynamics (CFD)-based modeling of journal bearings. The focus is on the steady-state characteristics (load capacity and equilibrium attitude curve). Three types of journal bearings are considered. Full 3D eccentric CFD models of the bearings are built in ANSYS CFX. Cavitation in the oil-lubricated hydrodynamic bearing is described using a two-phase homogeneous interface model. Custom scripts are developed to automate the procedure of finding the equilibrium position for given operating parameters through a series of steady-state CFD runs. Structural grids are used to discretize the lubricant flow region. The results are compared with available data obtained with the conventional methods of the analysis of journal bearings.

1 Introduction

In modern engineering, small-size high-speed turbomachinery is used in a continually expanding variety of applications. High-speed gas turbines, turbo-compressors, turbo-expanders, and turbo-generators are applied in power engineering, chemical and cryogenic industry, transport and marine engineering. In aerospace, the high-speed applications include turbopumps of liquid rocket engines, small-size gas turbine engines, turbo-generator-compressors for space power units, and turbo-expanders of aircraft air cycle machines.

Reliability of turbomachinery units depends largely on performance of the bearing supports. Standard rolling-element bearings have speed limits in terms of a parameter $D \times N$ (the product of bearing bore diameter in mm and shaft rotational speed in rpm) of about 2×10^6 mm/min. Even high-speed rolling-element bearings with silicone nitride balls continuously operating at several millions $D \times N$ may have the life time of hours and minutes.

Application of journal bearings with liquid or gaseous lubrication allows raising the parameter $D \times N$ by several times with simultaneous increase of service life. Also, reliability of high-speed turbomachines can be increased by using journal bearings with increased damping capability. Known successful applications of fluid-flim/gas bearing technology demonstrate time to failure of tens of thousand of hours. The authors and their co-workers developed more than ten types of different turbomachines with journal bearings.

The standard method for predicting fluid-film bearing operating characteristics is based on the theory of lubrication [8]. The two-dimensional Reynolds' equation is used to obtain pressure distribution in the fluid film. Approaches with a different degree of complexity exist varying from the simple short and long bearing theories to sophisticated models of elastohydrodynamic lubrication. The fluid-film bearing models based on the Reynolds' equation are usually coupled with simplified boundary conditions (i.e. for taking into account cavitation) and suitable semi-empirical expressions to cover turbulence effect. The lubrication theory models were proved valid for many fluid-film bearing applications. However, further development of the fluid-film and gas bearing technology in regard of current demands, especially towards the concept of oil-free turbomachinery (application of foil air bearings), requires the development and use of more comprehensive models with less fundamental assumptions.

Several works were focused on the validity of the Reynolds' equation (e.g., [1, 5]). An alternative, more general approach for the analysis of fluid-film bearings is based on the bulk-flow theory (e.g., [12, 13, 7]) and is also widely used in academia and industry.

Application of the computational fluid dynamics (CFD) methods for modeling journal bearings of various designs was studied in many works in the past (e.g., [15]). However, due to their considerable computational costs the CFD methods have not yet found wide application in journal bearing analysis.

Comparison between the codes for bearing analysis and a commercial general-purpose CFD package was presented in [6], where the static, dynamic, and thermal characteristics of hydrostatic and hydrodynamic oil bearings were studied. A heavy-loaded large-diameter oil bearing was analyzed in [16] using a free and open source CFD toolbox OpenFOAM.

This paper describes the process of prediction of operational characteristics of journal bearings using computational fluid dynamics methods. Three-dimensional Reynolds-Averaged-Navier-Stokes analysis is performed with the ANSYS CFX software package. The work considers three well-known bearing types (plain cylindrical hydrodynamic oil- and gas-lubricated bearings and hydrostatic water-lubricated bearing).

2 Geometric Parameters of Bearings

Geometric parameters of the considered radial journal bearings are listed in Table 1. Schematics of the oil and water bearings are shown in Figure 1. The geometrical models of all three bearings include the downstream regions at the left and right outlets of the bearings.

Table 1 Geometric parameters of the studied journal bearings

Parameter		Bearing type		
		Oil	Gas	Water
D	[mm]	55.00	50.00	40.0
D_2	[mm]	68.00	54.00	45.0
C	[mm]	0.075	0.02	0.075
L	[mm]	70.00	50.00	66.0
L_2	[mm]	80.00	50.00	66.0
d	[mm]	7.20	—	2.0
ℓ	[mm]	18.00	—	6.0
C_r	[mm]	—	—	1.0
w_r	[mm]	—	—	8.0
ℓ_r	[mm]	—	—	46.0

The oil bearing is a hydrodynamic bearing with one orifice located in the top arc of the bearing (see Figure 1).

The gas bearing has the simple geometry of axially-fed plain cylindrical aerodynamic bearing with much smaller radial clearance as compared to the fluid-film bearings.

The water bearing is a hydrostatic bearing with four rectangular inlet recesses (see Figure 1). Due to the large zones of small clearance between the recesses the water bearing can be considered as a hybrid bearing, which has both hydrostatic and hydrodynamic components of the load capacity at high rotational speeds.

3 CFD Model and Boundary Conditions

A commercial general-purpose CFD code ANSYS CFX is used to perform the analysis [2].

A full three-dimensional eccentric rotor analysis of the studied bearings incorporates a CFD model based on the Reynolds-Averaged-Navier-Stokes equations. The Shear Stress Transport (SST) model with automatic wall functions is used for turbulence treatment.

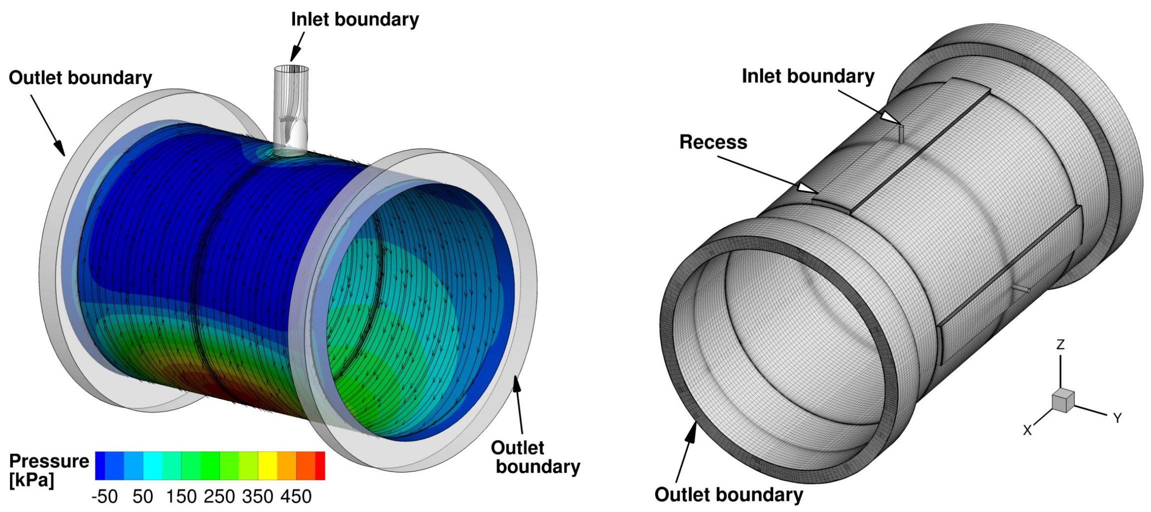

Fig. 1 Schematics of hydrodynamic oil bearing (left) and hydrostatic water bearing (right)

The pressure differential is set between the inlet and outlet boundaries. Boundary conditions at the outlet boundaries are treated as opening conditions. Rotational speed is defined on the shaft surface.

Steady-state simulations are performed with a pseudo-transient coupled CFX solver. High resolution advection scheme is used. Calculations for the high-eccentricity cases are performed with double precision.

Numerical convergence is checked by setting targets for the equation residuals and global balances. Physical convergence criteria imply constancy of maximal pressure, maximal gas content (for the cavitated oil bearing), and forces arising in the fluid film.

All three bearings are modeled using similar framework. Specific features of the models are described below.

3.1 Oil Bearing

Oil film is modeled as incompressible medium taking into account cavitation effects.

The oil density is 820 kg/m^3. Dependency of the oil dynamic viscosity on the oil temperature is taken into account by the following expression (dynamic viscosity is in [Pa·s], oil temperature is in [K])

$$\mu = \frac{-8.589 \times 10^{-4} T + 0.6034}{T - 282.7} \tag{1}$$

The operating regimes of the oil hydrodynamic bearing may include operation under cavitated conditions. Cavitation is the phenomenon of rupture of liquid phase and formation of gaseous cavities due to decrease in pressure at constant temperature. Cavitation can be divided into gaseous (due to ventilation from the surroundings, emission of gases dissolved in the liquid phase) and vaporous (phase change) cavitation. However, conventional simplified approaches used in the journal bearing models do not distinguish between the two types of cavitation. A recent review on the cavitation in journal bearings can be found in [3].

Cavitation of the oil film is modeled using a two-phase homogeneous interface model with a predefined saturation pressure. A differential transport equation is introduced for volume vapor fraction. The Rayleigh-Plesset equation is used to describe the mass transfer terms associated with grow and collapse of gas bubbles.

The gaseous phase is considered to be air. The mean bubble diameter required for the applied cavitation model is set to be 2.0×10^{-3} mm.

Shaft rotational speed is set to 1000 rpm for the oil bearing. Pressure drop is 1.0 bar.

3.2 Gas Bearing

The air flow in the aerodynamic gas bearing is modeled as compressible flow with the Thermal

Energy formulation. Ideal gas law is used for air at ambient temperature. Static pressure value of 1.0 bar is set on both opening boundaries of the gas bearing.

Shaft rotational speed for the gas bearing is calculated from the bearing number defined as

$$\Lambda = \frac{6\mu\omega}{p_a}\left(\frac{0.5D}{C}\right)^2 \tag{2}$$

The rotational speed values are in the range of 6700 rpm to 135 280 rpm.

3.3 Water Bearing

The water hydrostatic bearing is assumed to operate at constant pressure supply.

Water film is modeled as incompressible isothermal medium. Water properties are taken at the ambient temperature of 25°C.

The total pressure of 6.0 bar is set at the orifice inlets. Ambient static pressure is set at the outlet boundaries. Two rotational speed cases (7000 rpm and 15000 rpm) are considered.

3.4 Grid Generation

Generation of computational grids is performed in a commercial software ANSYS ICEM CFD.

Structured hexahedral O-grids are used in the analysis. Depending on the shaft position, recalculation of the clearance geometry, regeneration of the mesh and check of the grid quality are performed automatically for all types of the studied bearings. Such automation realized by tcl/tk scripts in ICEM CFD simplifies greatly the process of determination of the journal attitude curves.

Results of the grid independence study performed for the oil bearing were reported in [11]. It was shown that even as dense grids as about 77 million nodes demonstrated visible deviation in the maximum peak of pressure in the oil film. Using that data and based upon a trade-off between the computational costs and required accuracy the following computational meshes believed to provide sufficiently grid-independent results are applied in the analysis: 4 662 240 nodes for the oil bearing, 7 880 016 nodes for the gas bearing, and 3 299 256 nodes for the water bearing. Computation mesh for the water bearing is shown in Figure 1.

3.5 CFD Simulation

CFD simulations are performed for different cases of steady load and shaft rotational speed. The magnitude of the load is simulated by changing the eccentricity of the shaft in two directions. The main interest of this study is in predicting the journal attitudes curves, i.e. functions of the journal steady-state position at various vertical loads.

The approach of finding the steady-state position for a given load is based on the iterative correction of the rough estimation of the shaft eccentricity until the target load value is reached. The search process is to stop when the hydrodynamic reaction on the shaft is zero (within a tolerance) in the horizontal direction and equals to the predefined value in the vertical direction.

4 Lubrication Theory

The bearings are also modeled with the conventional lubrication theory to compare the predictions by both approaches.

In the lubrication theory the fluid film flow in the journal bearings is described by the two-dimensional Reynolds' equation. The Reynolds' equation takes into account turbulence in the film by using semi-empirical correlations for the turbulence factors (Constantinescu's model).

The Reynolds' equation is solved numerically using the finite element method on the structural uniform mesh of rectangles. The hydrodynamic reaction of the bearing is determined by integrating the pressure distribution p on the bearing surface.

Fluid-film rupture appearing in the divergent zone of the bearing clearance (negative pressure region) is taken into account by simple boundary conditions. The lubrication theory model is implemented in the in-house code for the journal bearing analysis running in MATLAB. Details on the used lubrication theory model can be found in [10].

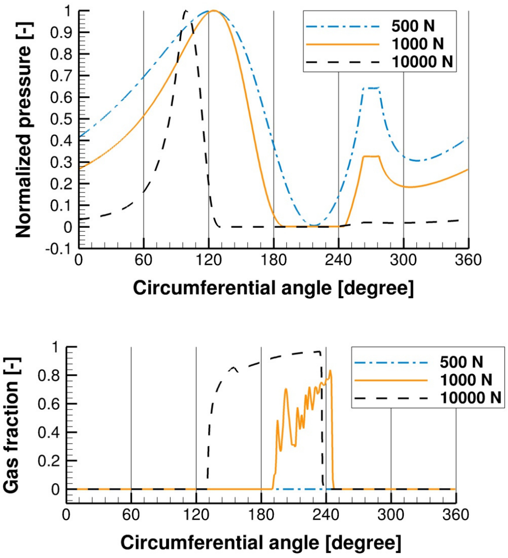

Fig. 2 Predicted Flow Characteristics in the Oil Bearing for Different Loads

5 Analysis of the Results

This section summarizes the numerical results obtained for the three studied bearings. The calculations are performed on a multi-core desktop computer with 128 GB of memory.

5.1 Oil Bearing

Typical pressure distribution and streamlines in the oil bearing are shown in Figure 1. Distributions of pressure and volume fraction of gaseous phase at the middle section of the bearing are shown in Figure 2 for different loads. Pressure magnitude is shown as ratio of the absolute pressure to the maximum pressure in the film. The circumferential position of the single orifice can be clearly identified from the pressure distribution curve for the small loads. Substantial cavitation occurs at the load of 1000 N and higher. As the load increases the cavitating zone expands in the direction of the smallest clearance.

The predicted journal attitude curve obtained by approximating calculated cases of different loads is shown in Figure 3. The dashed curve demonstrate the stator surface.

Comparison with the predictions by the Reynolds' equation is demonstrated in Figure 4 in terms of dimensionless load factor Φ_W, which

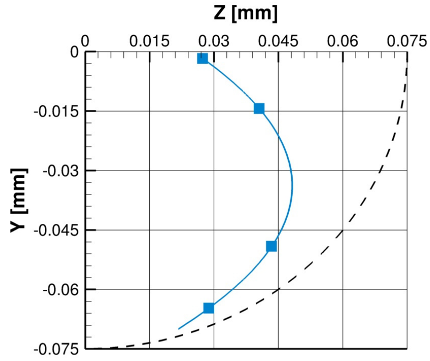

Fig. 3 Predicted Journal Attitude Curve for the Oil Bearing

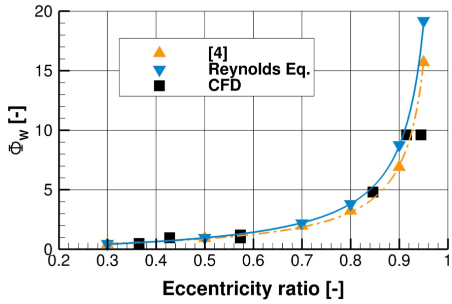

Fig. 4 Comparison with the Lubrication Theory for the Oil Bearing

is inversely proportional to the duty parameter

$$\Phi_W = \frac{\psi^2 W}{LD\mu\omega} \tag{3}$$

where $\psi = 2C/D$ is eccentricity ratio.

Data from the classical textbook [4] is also shown in Figure 4. All approaches provide similar results at small and medium eccentricity ratios. The deviations occur at high eccentricities, where the CFD model tends to predict lower values of the duty parameters as compared to the simplified methods.

5.2 Gas Bearing

Modeling of the aerodynamic gas bearing is performed for the different values of the bearing number Λ.

Comparison with the predictions by the Reynolds' equation is shown in Figure 5 in terms

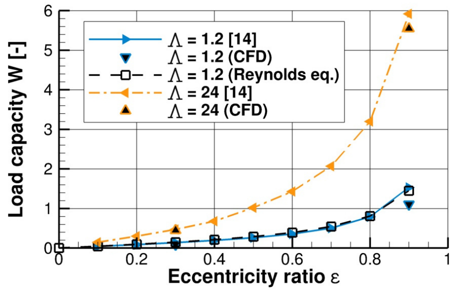

Fig. 5 Comparison with the Lubrication Theory for the Gas Bearing

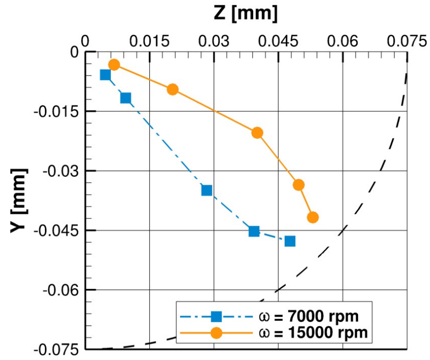

Fig. 6 Predicted Journal Attitude Curve for the Water Bearing

of the dimensionless load capacity

$$\overline{W} = \frac{W}{p_a DL} \tag{4}$$

Again, data from the classic textbook on aerodynamic bearings [14] is also shown.

Results obtained with the in-house code for solving Reynolds' equation are shown only for the case $\Lambda = 1.2$. The predictions are in good agreement, though the Reynolds' equation overpredicts the bearing load capacity at high eccentricity ratio compared to the CFD results. The Reynolds' equation results are virtually identical to those taken from [14].

5.3 Water Bearing

The journal attitude curves calculated for the water bearing are shown in Figure 6. Two cases of different rotational speed are presented.

At the rotational speed of 7000 rpm the attitude curve shape is close to a line starting from the center of the bearing, which is typical for the hydrostatic bearings lubricated by incompressible fluid [9, 12].

At the higher rotational speed the journal produces the hydrodynamic effect comparable with the hydrostatic reaction. The hydrostatic bearing operates in the hybrid mode. Therefore the journal attitude curve becomes more nonlinear.

6 Conclusions

The CFD-based modeling of the fluid-film and gas bearings is very time consuming as compared to the bearing analysis based on the Reynolds' equation. Nevertheless, using an automation of the CFD analysis (pre-processing, solving, and post-processing) makes it possible to reduce significantly time and effort necessary for the calculation of journal bearing operational characteristics.

The CFD predictions demonstrate good correlation with the available data for both oil and gas journal bearings studied in this work. However, as expected, deviations between the theoretical approaches are observed for the journals operating at high eccentricities and high rotational speeds.

The developed CFD models can now be applied for further studies on advanced journal bearing technology. In particular, the aerodynamic gas bearing model can be extended to model foil air bearings, for which an additional limitation of using Reynolds' equation is connected with large differences in the radial clearance between the shaft and the foils. Also, the developed models can be coupled with an appropriate method for determining rotordynamic coefficients of the bearings. This is, however, beyond the scope of this work.

References

[1] Almqvist T and Larsson R. Some remarks on the validity of Reynolds equation in the modeling of lubricant film flows on the surface roughness scale. *ASME J. Tribology*, Vol. 126, pp. 703-710, 2004.

[2] ANSYS, Inc. *ANSYS CFX-Solver theory guide*. Release 14.5, 2012.

[3] Braun MJ and Hannon WM. Cavitation formation and modelling for fluid film bearings: a review. *Proc. IMechE, Part J: J. Engineering Tribology*, Vol. 224, pp. 839-863, 2010.

[4] Chernavsky SA. *Journal bearings*. Moscow: Mashgiz, 1963. (In Russian)

[5] Dobrica MB and Fillon M. About the validity of Reynolds equation and inertia effects in textured sliders of infinite width. *Proc. IMechE, Part J: J. Engineering Tribology*, Vol. 223, pp. 69-78, 2009.

[6] Guo Z, Hirano T and Kirk RG. Application of CFD analysis for rotating machinery—Part I: Hydrodynamic, hydrostatic bearings and squeeze film damper. *ASME J. Eng. Gas Turbine Power*, Vol. 127, pp 445-451, 2005.

[7] Hélène M, Arghir M. and Frêne J. Combined Navier-Stokes and bulk-flow analysis of hybrid bearings: radial and angled injection. *ASME J. Tribology*, Vol. 127, pp. 557-567, 2005.

[8] Lang OR, and Steinhilper W. *Gleitlager*. Springer-Verlag, 1978.

[9] Peeken H. Hydrostatische Querlager. *Konstruktion*, Vol. 16(7), pp. 266-276, 1964.

[10] Pugachev AO, Tykhomirov VV, Sheremetyev AV, Spilenko OI and Timchenko ID. Sensitivity analysis of squeeze film dampers using Reynolds equation. *Proc 8th IFToMM International Conference on Rotor Dynamics*, KIST, Seoul, Korea, TuC1-3, pp. 454-462, 2010.

[11] Pugachev AO, Ravikovich YA, Ermilov YI, Kholobtsev DP and Matushkin AA. CFD-based modeling of oil and gas journal bearings using commercial software packages. *Vestnik of Samara State Aerospace University*, No. 41(3), pp. 211-220, 2013. (In Russian.)

[12] San Andrés L, Childs D and Yang Z. Turbulent-flow hydrostatic bearings: Analysis and experimental results. *Int. J. Mech. Sci.*, Vol. 37, pp. 815-829, 1995.

[13] San Andrés L. Bulk-flow analysis of hybrid thrust bearings for process fluid applications. *ASME J. Tribology*, Vol. 122, pp. 170-180, 2000.

[14] Sheinberg SA et al. *Gas-lubricated journal bearings*. Moscow: Mashinostroenie, 1979. (In Russian)

[15] Tucker PG and Keogh PS. A generalized computation fluid dynamics approach for journal bearing performance prediction. *Proc. IMechE, Part J: J. Engineering Tribology*, Vol. 209, pp. 99-108, 1995.

[16] Uhkoetter S, aus der Wiesche S, Kursch M and Beck C. Development and validation of a three-dimensional multiphase flow computational fluid dynamics analysis for journal bearings in steam and heavy duty gas turbines. *ASME J. Eng. Gas Turbine Power*, Vol. 134, pp. 102504-8, 2012.

Nomenclature

C	=	Radial clearance
C_r	=	Recess depth
D	=	Bearing diameter
D_2	=	Downstream region diameter
d	=	Orifice diameter
$D \times N$	=	Bearing speed factor
L	=	Bearing length
ℓ	=	Orifice length
ℓ_r	=	Recess axial length
L_2	=	Shaft length
p	=	Pressure
p_a	=	Ambient pressure
T	=	Temperature
W	=	Load capacity
w_r	=	Recess width
Λ	=	Bearing number
μ	=	Dynamic viscosity
ρ	=	Density
Φ_W	=	Load factor
ψ	=	Eccentricity ratio
ω	=	Rotational speed

7 Contact Author Email Address

yurav@mai.ru

Copyright Statement